

Core level excitation spectra of La and Mn ions in $LaMnO_3$

Fujian Li(李福建), Xinlu Cheng(程新路), and Hong Zhang(张红)

Citation: Chin. Phys. B, 2024, 33 (**3**): 033201. DOI: 10.1088/1674-1056/acfaf5
Journal homepage: http://cpb.iphy.ac.cn; http://iopscience.iop.org/cpb

What follows is a list of articles you may be interested in

L-shell x-ray fluorescence relative intensities for elements with 62 ≤ *Z* ≤ 83 at 18 keV and 23 keV by synchrotron radiation

M Alqadi, S AL-Humaidi, H Alkhateeb, and F Alzoubi
Chin. Phys. B, 2023, 32 (**8**): 083201. DOI: 10.1088/1674-1056/accb46

Electron emission induced by keV protons from tungsten surface at different temperatures

Li-Xia Zeng(曾利霞), Xian-Ming Zhou(周贤明), Rui Cheng(程锐), Yu Liu(柳钰), Xiao-An Zhang(张小安), and Zhong-Feng Xu(徐忠锋)
Chin. Phys. B, 2022, 31 (**7**): 073202. DOI: 10.1088/1674-1056/ac632f

Nd *L*-shell x-ray emission induced by light ions

Xian-Ming Zhou(周贤明), Jing Wei(尉静), Rui Cheng(程锐), Yan-Hong Chen(陈燕红),Ce-Xiang Mei(梅策香), Li-Xia Zeng(曾利霞), Yu Liu(柳钰), Yan-Ning Zhang(张艳宁), Chang-Hui Liang(梁昌慧), Yong-Tao Zhao(赵永涛), and Xiao-An Zhang(张小安)
Chin. Phys. B, 2022, 31 (**6**): 063204. DOI: 10.1088/1674-1056/ac4488

X-ray emission for Ar^{11+} ions impacting on various targets in the collisions near the Bohr velocity

Xian-Ming Zhou(周贤明), Jing Wei(尉静), Rui Cheng(程锐), Yan-Hong Chen(陈燕红), Ce-Xiang Mei(梅策香), Li-Xia Zeng(曾利霞), Chang-Hui Liang(梁昌慧), Yao-Zong Li(李耀宗), Yong-Tao Zhao(赵永涛), and Xiao-An Zhang(张小安)
Chin. Phys. B, 2021, 30 (**8**): 083201. DOI: 10.1088/1674-1056/abe22f

Extreme ultraviolet and soft x-ray spectral lines in Rb XXIX

Indu Khatri, Arun Goyal, Sunny Aggarwal, A K Singh, Man Mohan
Chin. Phys. B, 2016, 25 (**3**): 033201. DOI: 10.1088/1674-1056/25/3/033201

Core level excitation spectra of La and Mn ions in $LaMnO_3$

Fujian Li(李福建), Xinlu Cheng(程新路), and Hong Zhang(张红)[†]

Institute of Atomic and Molecular Physics, Sichuan University, Chengdu 610065, *China*

(Received 28 June 2023; revised manuscript received 14 September 2023; accepted manuscript online 19 September 2023)

Manganese-based perovskite is popular for research on ferromagnetic materials, and its spectroscopic studies are essential for understanding its electronic structure, dielectric, electrical, and magnetic properties. In this paper, the *M*-edge spectra of La ions and the *M*-edge, *L*-edge, and *K*-edge spectra of Mn ions in $LaMnO_3$ are calculated by considering both the free-ion multiplet calculation and the crystal field effects. We analyze spectral shapes, identify peak origins, and estimate the oxidation states of La and Mn ions in $LaMnO_3$ theoretically. It is concluded that La ions in $LaMnO_3$ predominantly exist in the trivalent state, while Mn ions exist primarily in the trivalent state with a minor presence of tetravalent ions. Furthermore, the calculated spectra are in better conformity with the experimental spectra when the proportion of Mn^{3+} is 90% and Mn^{4+} is 10%. This article enhances our comprehension of the oxidation states of La and Mn within the crystal and also provides a valuable guidance for spectroscopic investigations of other manganates.

Keywords: lanthanum manganate, the core level excitation spectra, free-ion multiplet calculation, oxidation state

PACS: 32.30.Rj, 61.05.cj, 78.70.Dm **DOI:** 10.1088/1674-1056/acfaf5

1. Introduction

The manganese-based perovskite $LaMnO_3$ has garnered significant attention due to its numerous applications in various fields, including solid-oxide fuel cells, electrocatalysis, supercapacitors, and colorimetric sensing.[1–6] As a type of A-type antiferromagnetic material, the Néel temperature of $LaMnO_3$ is $\sim$ 141 K,[7] and various interesting phenomena have been discovered and reported, such as colossal magnetoresistance effects,[8] exchange bias in superlattices[9] and orbital ordering,[10,11] indicating its great potential for use in the field of materials science. The spectral analysis is essential for understanding the electronic structure of $LaMnO_3$. X-ray photoelectron spectroscopy (XPS) and x-ray absorption spectroscopy (XAS) are typical spectral analysis methods. They can provide information on the reducibility, oxygen vacancies, and oxidation state of metal elements of perovskite oxides, which are important properties arising from structural features.

Accurate spectral simulations can be used not only to identify electronic structures but also to distinguish clearly between electronic and geometric effects on the spectral shape and edge position.[12] In recent decades, many theoretical approaches have been used to simulate $LaMnO_3$ transition spectra. A study by Elfimov *et al.* revealed that the polarization dependence of *K*-edge scattering is mainly caused by 4p orbital effects and energy band structure effects.[11] Ravindran *et al.* examined the ground and excited state properties of $LaMnO_3$ through full-potential calculations, successfully simulating the XANES spectra and determining the respective contribution of different elemental components to the spectral intensity within distinct energy ranges near the Fermi surface.[13] Based on the dipole approximation, Takahashi *et al.* calculated the *K*-edge absorption spectrum of Mn and observed that the spectral intensity increased with local lattice distortion and is not sensitive to the magnetic order.[14] Taguchi *et al.* calculated the Mn $L_{2,3}$-edge scattering and absorption spectra in MnO_6 using a cluster model that considered the Mn intra-atomic multiplet state coupling.[15] According to their findings, the intensity of the L_3-edge is strongly associated with the Jahn–Teller distortion, while the intensity of the L_2-edge is closely correlated with the orbital ordering. Moreover, numerous theoretical approaches have been employed to calculate the near-edge structure of transition metals. For instance, Pinjari *et al.* simulated the XAS of iron *L*-edges using the multiconfigurational wavefunction theory.[16] The *L*-edge spectra of transition metals were calculated with the CTM4XAS program package by Stavitski *et al.*[17] de Groot *et al.* reviewed a series of principles and methods for calculating the 2p x-ray absorption spectra of transition metals, considering atomic multiplet effects, charge transfer effects, crystal field effects, and x-ray magnetic circular dichroism.[18]

The investigation of the valence state of Mn in manganese-based perovskites is significant. The Mn 3d orbitals undergo energetic degeneracy with O 2p orbitals, resulting in strong covalent interactions, which determine the formation of electronic structures and ferromagnetism.[5] Zhang *et al.* conducted experiments to explore the lanthanum–oxygen and manganese–oxygen interaction in $LaMnO_3$. Their findings confirmed that lanthanum is present in a +3 valence state, while manganese exists in both +3 and +4 valence states, excluding the +2 valence state.[19–21] Valmor *et al.* investigated the local structure of the Mn site in the $LaMnO_3$ sample us-

[†]Corresponding author. E-mail: hongzhang@scu.edu.cn

© 2024 Chinese Physical Society and IOP Publishing Ltd

ing Mn K-edge x-ray absorption spectroscopy and showed that the Mn ions are at the intermediate oxidation state with an average valency of +3.4.[22] Depending on the valence state of manganese atoms, temperature and pressure, they exhibit different electrical and magnetic phases, including antiferromagnetic insulators or ferromagnetic-metallic, and also exhibit charge-orbit ordered phases.[5,23,24] $LaMnO_3$ usually has an Mn^{3+}–O–Mn^{4+} double exchange caused by the cation deficiency, which increases the average valence of Mn ions.[25] Under an oxygen-excess environment, the content of Mn^{4+} increases as the oxygen vacancy decreases, resulting in an elevation of the average valence of Mn ions in $LaMnO_3$, thereby facilitating the formation of mixed valence states. The strong tilting of the MnO_6 octahedra with respect to the ideal cubic perovskite structure and the remarkable distortion of the lattice by the Jahn–Teller (JT) effect leads to a change in the oxidation state of the Mn. In addition, many studies have demonstrated that proper doping of metal cations (e.g., Sr, Ba, and Ca) in $LaMnO_3$ can regulate the valence of Mn ions and enhance the electronic, magnetic, and transport properties of the material.[22,26,27]

The spectra show different features with different valence states of La and Mn in $LaMnO_3$. The 3d spectrum of La shows well spin–orbit splitting, and the binding energy of La^{2+} is shifted 3.1 eV lower than that of La^{3+}. For Mn ions, the spectrum exhibits exchange splitting on the M-edge, and the magnitude of this splitting energy shows a certain linear relationship with the valence of the Mn ion.[28] In the $L_{2,3}$-edges and K-edges, the spectrum shifts toward higher energy as the valence of the Mn ion increases.[27,29] The values of the white-line intensity ratio (L_3/L_2) and spin–orbit splitting on the $L_{2,3}$-edges depend on the valence of the Mn ion.[30,31] This article adopts a calculation method based on configuration interaction, which successfully avoids the interference of other ions on the x-ray absorption spectrum of the central ion in the experiment spectrum. As a result, more accurate ion spectral data was obtained. The origin of spectral peaks in $LaMnO_3$ crystals was identified through x-ray spectroscopy, and the oxidation states of La and Mn in $LaMnO_3$ were analyzed in detail. This helps us understand the electronic and geometric structure information of the material, and may also provide a new perspective for explaining some phenomena caused by the structural characteristics inside $LaMnO_3$. In addition, identifying the redox states of Mn and La ions in $LaMnO_3$ can provide valuable insights into the electrochemical properties, which can be used to design and optimize material catalytic performance.

We organize the article as follows. A description of the computational methods is given in Section 2, which contains both atomic multiplet calculations and crystal field multiplet calculations. The M-edge spectra of La ion, M-edge, L-edge and K-edge spectra of Mn ion in $LaMnO_3$ are discussed in Section 3 respectively. A conclusion is given in Section 4. The experimental spectra compared with this article were obtained by XAS and XPS.[27,28,32–35]

2. Methods

2.1. Free-ion multiplet calculation

A series of calculations were performed using the flexible atomic code (FAC) program for the transition spectra of the La M-edge, the Mn M-edge, $L_{2,3}$-edge, and K-edge. These calculations primarily involve excitations: La $3d^{10}4f^0 \rightarrow 3d^9 4f^1$; Mn $3s^2 3d^4 \rightarrow 3s^1 3d^5$, $2p^6 3d^4 \rightarrow 2p^5 3d^5$, $1s^2 3d^4 \rightarrow 1s^1 3d^5$, $1s^2 4s^0 \rightarrow 1s^1 4s^1$ and $1s^2 4p^0 \rightarrow 1s^1 4p^1$. The calculation of the multiple structure of the ionic core level is based on the configuration interaction of independent particle ground state wavefunctions. To account for the electronic screening effect resulting from the self-consistent field of the nuclear potential, the ground state wavefunction includes both the core potential and electron–electron interactions. The standard Dirac–Coulomb Hamiltonian is employed in the FAC, which thoroughly considers significant relativistic effects such as spin–orbit interactions and mass effects.[36] The standard jj-coupling mechanism is employed to simulate the transition spectra of La and Mn ions, and the Gaussian functions are used to fit the spectra in the MATLAB program.

The FAC program primarily investigates excitation transitions of free ions. However, in crystals, these transitions are additionally influenced by crystal field effects and interatomic interactions. In $LaMnO_3$ crystals, the Jahn–Teller effect changes the bond length of Mn–O in the MnO_6 octahedra, resulting in energy level shifts.[37,38] We considered the experimental spectrum of lanthanum oxide and manganese oxides to explain the deviations of experimental and calculated spectra of $LaMnO_3$.[19,20,34,39,40] Our calculations reveal that the energy deviation in the La ion spectrum is less than 0.5 eV, while in the Mn ion spectrum it ranges from 2.5 eV to 5 eV. This can be attributed to the comparatively weaker interaction between La ions and O ions in the crystal, in contrast to the interaction between Mn ions and O ions. Consequently, the spectrum of La ion in the crystal closely resembles that of free ions.

2.2. Crystal field multiplet calculation

In crystal field multiplet theory, the transition metal ion is treated as an independent particle surrounded by point charges, which effectively captures the symmetry of the intermediate ion.[41] The 3d orbital energy of the transition metal (Mn) ion is influenced by the octahedral arrangement of the six oxygen atoms. The cubic crystal field plays a crucial role in splitting the five 3d orbitals by symmetry into a two-fold degenerate E_g

($d_{x^2-y^2}$, $d_{3z^2-r^2}$) and a three-fold degenerate T_{2g} (d_{xy}, d_{yz}, and d_{xz}). The splitting between the E_g and T_{2g} orbitals is defined by the parameter 10 Dq, where E_g accounts for 6 Dq and T_{2g} for 4 Dq. The E_g orbital, oriented towards the oxygen ion in the octahedral environment, exhibits stronger antibonding interactions in comparison to the T_{2g} orbital situated between the oxygen ions, thereby leading to its elevated energy state. The crystal field within the perovskite structure originates from covalent interactions with neighboring oxygen atoms, with the E_g orbitals exhibiting stronger hybridization characteristics than the T_{2g} orbitals. The existence of a large crystal field splitting indicates a high degree of hybridization, with typical splitting distances ranging from 1 eV to 2 eV.[18,42]

3. Results and discussion

3.1. Spectral study for *M*-edge of Mn in $LaMnO_3$

In terms of shallow-core spectroscopy, Sen Gupta *et al.* propose a theory about the valence excitation of shallow-core between orbitals of the same principal quantum.[43] Their theory implies that the energy of the multipole transition corresponding to the bound state is lower than that of the dipole transition. This transition can be effectively simulated by the local single-ion model.[44] The spectral line with energy between 78 eV and 94 eV corresponds to the excitation of Mn^{3+}: $3s^23d^4 \rightarrow 3s^13d^5$, which is a quadrupole transition. The calculated results are shown in Fig. 1.

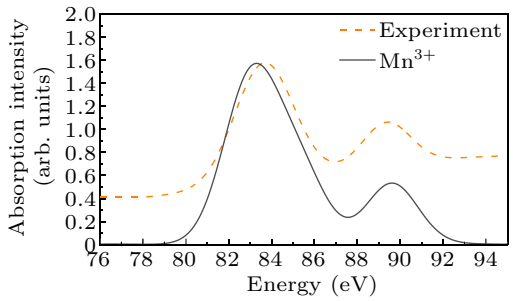


Fig. 1. The calculated and experimental spectra at the *M*-edge of Mn^{3+} in $LaMnO_3$.

In the 3s core-level spectral of manganese ions, an exchange splitting is detected with a size of $(2S+1)G^2(3s,3d)/5$, where S is the local spin of the ground state 3d electron, and $G^2(3s,3d)$ is the Slater exchange integral between 3s and 3d electrons.[45,46] The exchange splitting of Mn^{3+} is about 5.5 eV, but this value decreases as the Mn oxidation state increases.[28] Meanwhile, the presence of Mn^{2+} and Mn^{4+} during the experimental procedure has an impact on the spectra. In conclusion, free-ion multiplet calculations serve as a valuable tool in identifying Mn ion spectra, and the calculated spectrum matches the experimental spectrum closely.[47]

3.2. Spectral study for *M*-edge of La in $LaMnO_3$

The oxidation state of La in $LaMnO_3$ was determined by analyzing the *M*-edge spectra of La ions. Figure 2 compares the calculated spectra of La^{2+} and La^{3+} ions and the experimental spectra of La in $LaMnO_3$. The spectra with energies between 825 eV and 860 eV are produced by electron transition from La 3d to La 4f orbitals. The transition spectra show that the relative intensity of La^{2+} is much greater than that of La^{3+}, and the bond energy of La^{2+} is 3.1 eV lower than that of La^{3+}. The peaks observed at 833.92 eV and 836.70 eV in the La^{3+} spectrum correspond to the splitting peaks of La $3d_{5/2}$, and the peaks at 850.73 eV and 853.09 eV correspond to La $3d_{3/2}$. The calculated spectrum of La^{2+} exhibits a spin–orbit splitting energy of 17.22 eV, whereas La^{3+} displays a spin–orbit splitting energy of 16.81 eV. The experimental spectrum of La_2O_3 exhibits comparable features to that of La^{3+}, further confirming the reliability of the accuracy of the calculation results.[19,20,40] We compare the experimental spectra of La in $LaMnO_3$ with the calculated spectra of La^{2+} and La^{3+}. The analysis showed that the experiment spectra agree with the calculated spectra of La^{3+} in terms of energy and shape. Consequently, it can be concluded that La in $LaMnO_3$ exists at a valence state of +3, which agrees with the results obtained by Flores-Lasluisa *et al.*[19,21,35,48] The experimental spectrum displays a discrepancy in multiple splitting values, which is 0.9 eV higher than the calculated value. This disparity can be attributed to the presence of lanthanide oxides in the experiment and the transfer of electrons from the oxygen center to the La 4f shell layer.[35,49]

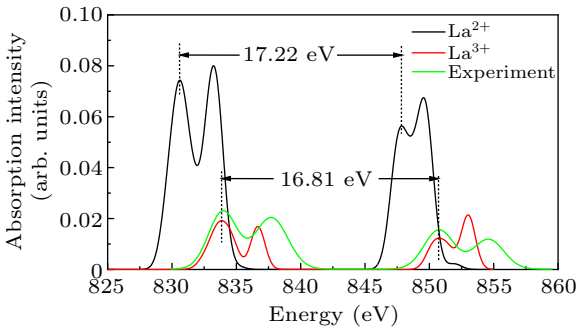


Fig. 2. The calculated spectra in *M*-edge of $La^{2+}$and La^{3+} and experimental spectra from XAS of $LaMnO_3$.

3.3. Spectral study for $L_{2,3}$-edge of Mn in $LaMnO_3$

Figure 3 shows the calculated spectrum of Mn^{3+} $L_{2,3}$-edge alongside the experimental spectrum of $LaMnO_3$. The spectral lines within the energy range of 635 eV to 660 eV are generated by the electron transition from Mn 2p orbitals to 3d orbitals. The Mn 2p core hole exhibits two broad multiplet states, namely, the high spin $2p_{1/2}$ state (L_2-edge) and low spin $2p_{3/2}$ state (L_3-edge), as a result of spin–orbit splitting. In addition, we incorporate crystal field corrections to account for the multiplet calculation of free ions, with a crystal field

splitting energy of 10 Dq = 2.0 eV for Mn. There are four possible transitions: $2p_{1/2} \rightarrow T_{2g}$, $2p_{1/2} \rightarrow E_g$, $2p_{3/2} \rightarrow T_{2g}$, and $2p_{3/2} \rightarrow E_g$. The interaction between the ligand and E_g orbitals is significantly stronger than that of T_{2g} orbitals in octahedral symmetry.[42] Therefore, the absorption peaks of E_g are higher than T_{2g} in the $L_{2,3}$-edge spectra. This is illustrated in Fig. 3, which showcases the enhanced resemblance between the ionic and crystal spectra resulting from the incorporation of the crystal field correction.

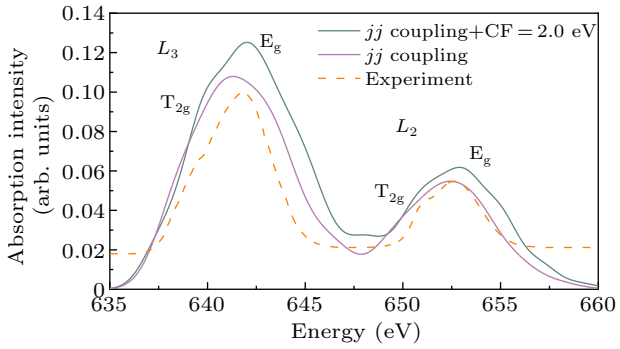


Fig. 3. The experimental spectra from XAS of $LaMnO_3$ and the calculated spectra in $L_{2,3}$-edge of Mn^{3+}: j–j coupling and j–j coupling + CF.

The influence of Mn^{2+}, Mn^{3+}, and Mn^{4+} on the $L_{2,3}$-edge spectrum varies, as depicted in Fig. 4. To facilitate a more accurate comparison with the experimental spectra, all calculated spectra have been adjusted by 2.5 eV towards the lower energy direction. The obtained spectra are consistent with those experimentally derived by Morales *et al.*[50,51] Two main factors are considered in this study. Firstly, the shape of the L_2-edge peak indicates a stronger agreement between the theoretical and experimental spectra for Mn^{3+} than for Mn^{4+}, while no agreement is observed for Mn^{2+}. Secondly, an increase in the valence state of the manganese ion leads to a shift in peak energy towards higher values. These descriptions suggest that the majority of the Mn ions in $LaMnO_3$ exist in the Mn^{3+} state, with a minor fraction in the Mn^{4+} state, while Mn^{2+} is insignificant.

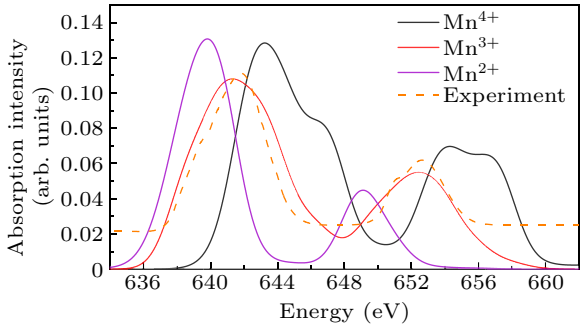


Fig. 4. The calculated spectrum in $L_{2,3}$-edge of Mn^{2+}, Mn^{3+}, and Mn^{4+} and experimental spectrum from XAS of $LaMnO_3$.

The $L_{2,3}$-edge spectrum of Mn is commonly employed in spectroscopy research for determining the valence state. Previous studies have documented various techniques for determining the oxidation state of Mn, with a focus on the shift of the peak toward higher energies as the Mn valence increases and the observed valence-dependent behavior of the L_3/L_2 white-line intensity ratio.[29–31] In our research, we calculated the spectrum of Mn^{3+} and found that the white line intensity ratio was 1.972:1, which is near the single-particle theoretical value of 2:1. This result further supports the reliability of the computational method. Additionally, we synthesized the calculated spectra of Mn in various proportions and compared them with the experimental spectra. Figure 5 shows that a high degree of agreement between the theoretical and experimental spectra was observed when Mn^{3+} is 90% and Mn^{4+} is 10%.

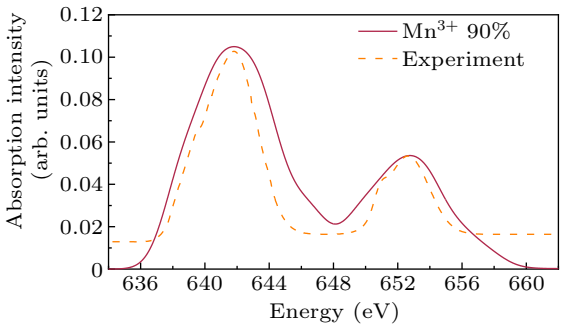


Fig. 5. The calculated spectrum in $L_{2,3}$-edge of Mn^{3+} and Mn^{4+} at different ratios and the experimental data for $LaMnO_3$.

3.4. Spectral study for *K*-edge of Mn in $LaMnO_3$

Figure 6 presents a comparative analysis of the K-edge spectrum of Mn^{2+}, Mn^{3+}, and Mn^{4+}. The spectrum shifts toward higher energies as the valence of Mn ions increases, making the K-edge spectrum a valuable tool for determining the valence of manganese in compounds.[27,52] Notably, the K-edge spectrum of Mn^{3+} is closest to the experimental spectrum in both shape and energy, while Mn^{4+} displays a lesser degree of overlap. Conversely, the K-edge spectrum of Mn^{2+} exhibits substantial deviation from the experimental spectrum, which echoes our conclusion in $L_{2,3}$-edge. Our analyses indicate that Mn^{3+} and Mn^{4+} are the primary oxidation states of Mn ions in $LaMnO_3$, while Mn^{2+} is not detected.

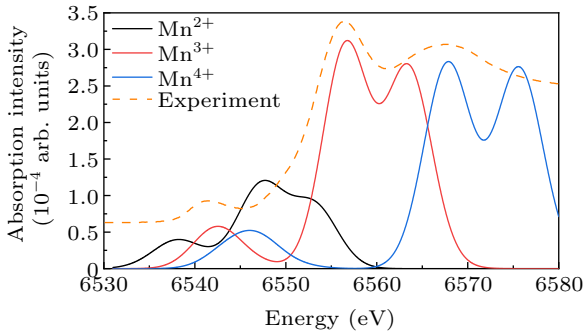


Fig. 6. Calculated spectrum in K-edge of Mn^{2+}, Mn^{3+}, and Mn^{4+} and experimental spectrum from XAS of $LaMnO_3$.

The ionic multiplet model allows us to identify spectral transitions that assist in analyzing the origin of the peaks. Specifically, in the K-edge spectrum of Mn^{3+}, the prepeak structure at 6542 eV is located about 14 eV below the main

K-edge peak of manganese. This structure corresponds to a quadrupole transition occurring from the 1s core level to the empty 3d level, which represents a dipole-forbidden transition and consequently exhibits limited intensity. Elfimov *et al.* has proposed the existence of a dipole contribution to the prepeak in $LaMnO_3$, which arises from the strong hybridization between the Mn 4p orbitals and the adjacent Mn atom's 3d orbitals facilitated by oxygen 2p orbitals.[11] The peak observed at 6556 eV corresponds to the excitation from 1s orbital to 4s orbital of Mn^{3+}, while the peak observed at 6563 eV corresponds to a dipole transition from 1s orbital to 4p orbital. Correspondingly, the peaks observed at energies of 6546 eV, 6567 eV, and 6575 eV can be attributed to the excitations of Mn^{4+} from the 1s orbital to the 3d, 4s, and 4p orbitals, respectively.

The influence of different ratios of Mn^{3+} and Mn^{4+} in $LaMnO_3$ on the *K*-edge spectra is simulated in Fig. 7. The results suggest that with an increasing proportion of Mn^{3+}, the prepeak A shifts to lower energy. Moreover, there is a discernible trend of intensity transfer from a relatively weaker peak B (compared to peak C) to a relatively stronger peak B (compared to peak C). The synthetic spectra show a significant degree of concordance with the experimental spectra when the proportion of Mn^{3+} falls within the range of 88%–90%. However, a discrepancy arises between the synthetic spectrum and the experimental spectrum at peak C. This discrepancy is attributed to the strong hybridization of the E_g orbitals in the 3d of Mn with the 2p orbitals of the adjacent O ions, which causes a broadening of the energy band within the solid.

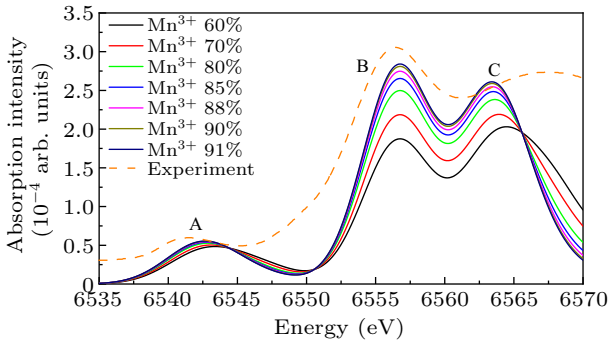


Fig. 7. The calculated spectrum of Mn^{3+} and Mn^{4+} at different ratios and the experimental spectrum for $LaMnO_3$.

There are several reasons for the appearance of mixed valence states of Mn ions in the $LaMnO_3$: (i) The material exhibits the presence of cationic defects, such as vacancies in La or Mn ions, which lead to the valence state of some Mn ions changing from +3 to +4 in order to maintain overall electrical neutrality. (ii) An excess of oxygen ions in the material, which presents in metal ion vacancies or lattice gaps. This excess of oxygen ions causes an increase in the valence of Mn ions. (iii) The crystal structure can be affected by deviations from standard stoichiometric ratios, as well as the temperature and duration of the annealing process during its preparation, which further changes the valence state of Mn ions.

4. Conclusion

The core electron excitation spectrums for La and Mn are calculated, and a theoretical estimation for determining the effective oxidation states of La and Mn in $LaMnO_3$ is provided. From the point of free ions, we analyzed the contribution of La and Mn ions in various valence states to the spectrum by considering that the spectral shapes and mainline positions are mainly influenced by the oxidation state of the central atom. The *M*-edge spectra of La demonstrate a concurrence between the experimental spectra and the calculated spectra of La^{3+} in terms of the spin–orbit splitting values and peak positions, indicating that the La ion is positively trivalent in $LaMnO_3$. However, the $L_{2,3}$-edge and *K*-edge spectra of Mn, clearly indicate the presence of a mixed valence state in $LaMnO_3$, predominantly composed of Mn^{3+} with a minor fraction of Mn^{4+}, while the absence of Mn^{2+} is evident. The synthetic spectrum at the $L_{2,3}$-edge aligns with the experimental spectrum when the Mn^{3+} content is 90% and Mn^{4+} is 10%, which is consistent with the Mn^{3+} proportions ranging from 88% to 90% obtained at the *K*-edge. The results also indicate that a weak interaction between lanthanum and manganese in $LaMnO_3$, while the interaction between manganese and oxygen is robust. This investigation enhances our ability to analyze crystal spectrum and deepens our understanding of the electronic structure information in perovskite materials.

Acknowledgment

Project supported by the National Natural Science Foundation of China (Grant No. 11974253).

References

[1] Labhasetwar N, Saravanan G, Megarajan S K, Manwar N, Khobragade R, Doggali P and Grasset F 2015 *Sci. Technol. Adv. Mater.* **16** 036002
[2] Tomar A K, Joshi A, Singh G and Sharma R K 2021 *Coord. Chem. Rev.* **431** 213680
[3] Wang Y, Chen L, Cao H, Chi Z, Chen C, Duan X, Xie Y, Qi F, Song W and Liu J 2019 *Appl. Catal. B* **245** 546
[4] Song L, Zhu Y, Yang Z, Wang C and Lu X 2018 *J. Mater. Chem. B* **6** 5931
[5] El Hannani M D, Rached D, Rabah M, Khenata R, Benayad N, Hichour M and Bouhemadou A 2008 *Mater. Sci. Semicond. Process.* **11** 81
[6] Mefford J T, Hardin W G, Dai S, Johnston K P and Stevenson K J 2014 *Nat. Mater.* **13** 726
[7] Matsumoto G 1970 *J. Phys. Soc. Jpn.* **29** 606
[8] Moritomo Y, Asamitsu A, Kuwahara H and Tokura Y 1996 *Nature* **380** 141
[9] Gibert M, Zubko P, Scherwitzl R, Íñiguez J and Triscone J M 2012 *Nat. Mater.* **11** 195
[10] Murakami Y, Hill J, Gibbs D, Blume M, Koyama I, Tanaka M, Kawata H, Arima T, Tokura Y and Hirota K 1998 *Phys. Rev. Lett.* **81** 582
[11] Elfimov I S, Anisimov V I and Sawatzky G A 1999 *Phys. Rev. Lett.* **82** 4264

[12] Li Y J, Haschaolu W, Wurentuya, Song Z Q, Ou Z Q, Tegus O and Ikuo N 2015 *Chin. Phys. B* **24** 086101

[13] Ravindran P, Kjekshus A, Fjellvåg H, Delin A and Eriksson O 2002 *Phys. Rev. B* **65** 064445

[14] Takahashi M, Igarashi J I and Fulde P 1999 *J. Phys. Soc. Jpn.* **68** 2530

[15] Taguchi M and Altarellli M 2002 *Surf. Rev. Lett.* **9** 1167

[16] Pinjari R V, Delcey M G, Guo M Y, Odelius M and Lundberg M 2014 *J. Chem. Phys.* **141** 124116

[17] Stavitski E and De Groot F M 2010 *Micron* **41** 687

[18] de Groot F M, Elnaggar H, Frati F, Wang R P, Delgado-Jaime M U, van Veenendaal M, Fernandez-Rodriguez J, Haverkort M W, Green R J and van der Laan G 2021 *J. Electron Spectrosc. Relat. Phenom.* **249** 147061

[19] Zhang C, Wang C, Zhan W, Guo Y, Guo Y, Lu G, Baylet A and Giroir-Fendler A 2013 *Appl. Catal. B* **129** 509

[20] Elsiddig Z A, Xu H, Wang D, Zhang W, Guo X, Zhang Y, Sun Z and Chen J 2017 *Electrochim. Acta* **253** 422

[21] Huang J, Teng Z, Kang R, Bin F, Wei X, Hao Q, Hui K N, Hui K S and Dou B 2021 *Fuel* **292** 120289

[22] Mastelaro V R, de Souza D P and Mesquita R A 2002 *X-Ray Spectrom.* **31** 154

[23] Sun Q, Luo X, Xia Q, Guo Y, Su J, Li Q and Miao G 2020 *J. Magn. Magn. Mater.* **499** 166317

[24] Tao Y M, Lin L, Dong S and Liu J M 2012 *Chin. Phys. B* **21** 107502

[25] Horyn R, Sikora A and Bukowska E 2003 *J. Alloys Compd.* **353** 153

[26] Abu-Samak M, Kumar U, Quraishi A, Kumar R, Kumar S, Dalela S, Ahmad M A, Choudhary B and Alvi P 2022 *Physica B* **628** 413562

[27] Pandey S, Bindu R, Kumar A, Khalid S and Pimpale A 2008 *Pramana* **70** 359

[28] Borca C N, Canulescu S, Loviat F, Lippert T, Grolimund D, Dobeli M, Wambach J and Wokaun A 2007 *Appl. Surf. Sci.* **254** 1352

[29] Delcey M G, Lindblad R, Timm M, Bulow C, Zamudio-Bayer V, von Issendorff B, Lau J T and Lundberg M 2022 *Phys. Chem. Chem. Phys.* **24** 3598

[30] Varela M, Oxley M P, Luo W, Tao J, Watanabe M, Lupini A R, Pantelides S T and Pennycook S J 2009 *Phys. Rev. B* **79** 085117

[31] Nishida S, Kobayashi S, Kumamoto A, Ikeno H, Mizoguchi T, Tanaka I, Ikuhara Y and Yamamoto T 2013 *J. Appl. Phys.* **114** 054906

[32] Saitoh T, Bocquet A E, Mizokawa T, Namatame H, Fujimori A, Abbate M, Takeda Y and Takano M 1995 *Phys. Rev. B* **51** 13942

[33] Cho D Y, Kim J Y, Park B G, Rho K J, Park J H, Noh H J, Kim B, Oh S J, Park H M and Ahn J S 2007 *Phys. Rev. Lett.* **98** 217601

[34] Stranick M A 1999 *Surf. Sci. Spectra (USA)* **6** 39

[35] Flores-Lasluisa J X, Huerta E, Cazorla-Amoros D and Moralion E 2022 *Energy* **247** 123456

[36] Gu M F 2008 *Can. J. Phys.* **86** 675

[37] Popovic Z and Satpathy S 2000 *Phys. Rev. Lett.* **84** 1603

[38] Jahn H A and Teller E 1937 *Proc. R. Soc. Lond. A-Math. Phys. Sci.* **161** 220

[39] Oku M, Hirokawa K and Ikeda S 1975 *J. Electron Spectrosc. Relat. Phenom.* **7** 465

[40] Li Y, Guan B, Maclennan A, Hu Y, Li D, Zhao J, Wang Y and Zhang H 2017 *Electrochim. Acta* **241** 395

[41] Bethe H 1929 *Ann. Phys.* **395** 133

[42] Degroot F M F, Fuggle J C, Thole B T and Sawatzky G A 1990 *Phys. Rev. B* **42** 5459

[43] Sen Gupta S, Bradley J A, Haverkort M W, Seidler G T, Tanaka A and Sawatzky G A 2011 *Phys. Rev. B* **84** 075134

[44] Ruotsalainen K O, Sahle C J, Ritschel T, Geck J, Hosoda M, Bell C, Hikita Y, Hwang H Y, Fister T T, Gordon R A, Hamalainen K, Hakala M and Huotari S 2015 *J. Phys. Condens. Matter* **27** 335501

[45] Zhao L Z and Young V 1984 *J. Electron Spectrosc. Relat. Phenom.* **34** 45

[46] Bocquet A E, Fujimori A, Mizokawa T, Saitoh T, Namatame H, Suga S, Kimizuka N, Takeda Y and Takano M 1992 *Phys. Rev. B* **45** 1561

[47] Zhao C, Zhang H and Cheng X 2022 *J. Solid State Chem.* **311** 123145

[48] Ma P, Lei N, Yu B, Liu Y, Jiang G, Dai J, Li S and Lu Q 2019 *Nanomaterials* **9** 1676

[49] Kucharczyk B and Tylus W 2007 *Catal. Lett.* **115** 122

[50] Morales F, de Groot F M F, Glatzel P, Kleimenov E, Bluhm H, Havecker M, Knop-Gericke A and Weckhuysen B M 2004 *J. Phys. Chem. B* **108** 16201

[51] Oishi M, Yamanaka K, Watanabe I, Shimoda K, Matsunaga T, Arai H, Ukyo Y, Uchimoto Y, Ogumi Z and Ohta T 2016 *J. Mater. Chem. A* **4** 9293

[52] Lafuerza S, García J, Subías G, Blasco J and Glatzel P 2016 *Phys. Rev. B* **93** 205108